NATIONAL ADVISORY COMMITTEE FOR AERONAUTICS

TECHNICAL NOTE 2195

A FLIGHT INVESTIGATION AND ANALYSIS OF THE LATERAL-

OSCILLATION CHARACTERISTICS OF AN AIRPLANE

By Carl J. Stough and William M. Kauffman

Ames Aeronautical Laboratory
Moffett Field, Calif.

NACA

Washington

October 1950

NATIONAL ADVISORY COMMITTEE FOR AERONAUTICS

TECHNICAL NOTE 2195

A FLIGHT INVESTIGATION AND ANALYSIS OF THE LATERAL-
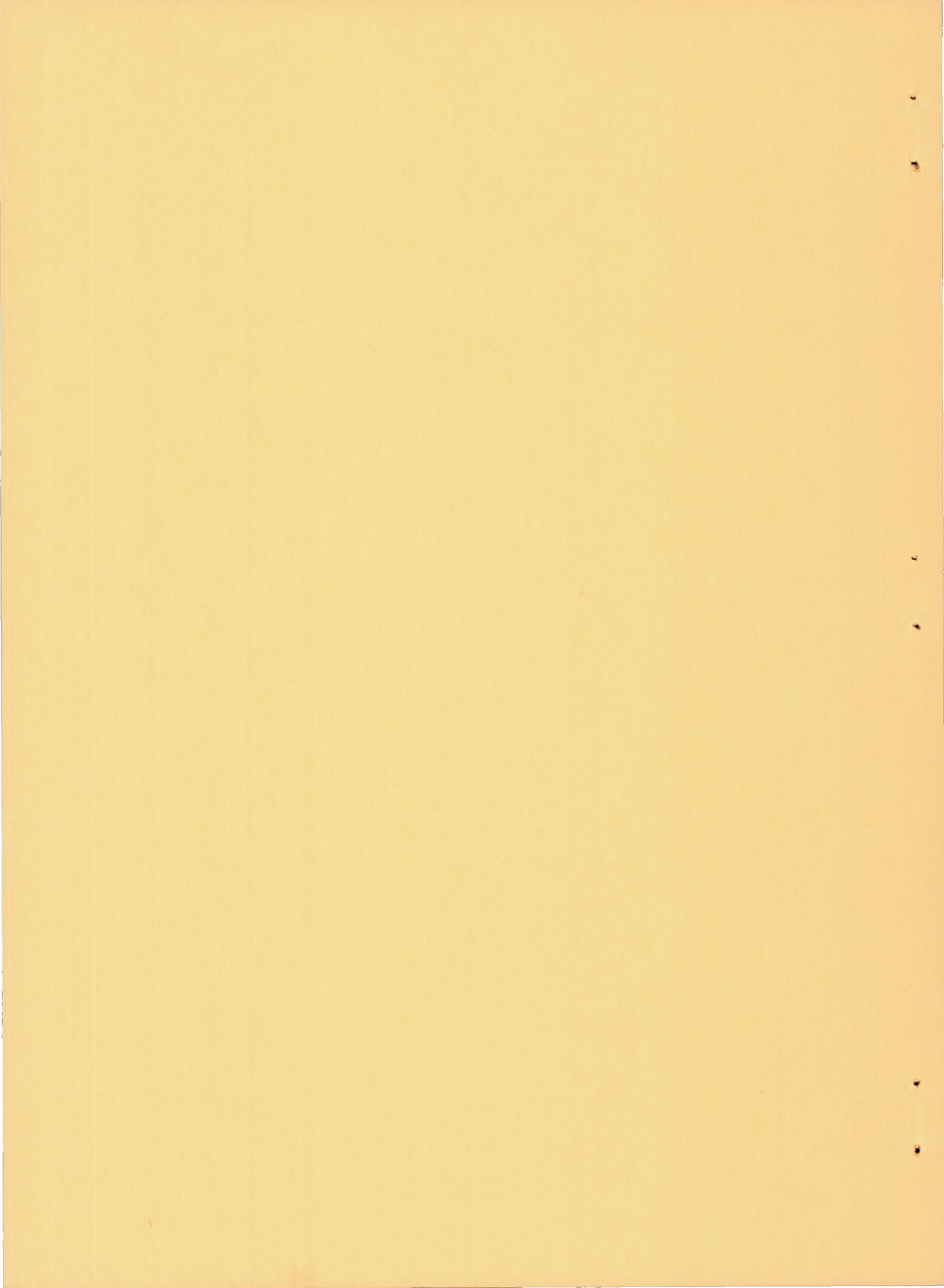
OSCILLATION CHARACTERISTICS OF AN AIRPLANE

By Carl J. Stough and William M. Kauffman

SUMMARY

Flight tests were conducted and an analysis made to determine the causes of undesirable dynamic lateral-stability characteristics of an airplane. Various rudder modifications were flight tested with the rudder free and fixed over an indicated airspeed range from approximately 200 to 450 miles per hour. Rudder-hinge-moment and other pertinent data were obtained by flight and wind-tunnel tests.

The oscillation period and time required to damp to one-half amplitude measured in flight are compared with calculated curves in which these characteristics are given as functions of the important rudder hinge-moment parameters.

An analysis of the data showed that there were no significant changes in the basic rudder-fixed stability derivatives with indicated airspeed, and the rudder-fixed damping characteristics were predictable with sufficient accuracy if the product-of-inertia terms were considered.

Freeing the rudder brought about a reduction in the damping of the oscillation at low speed; this is attributed to the low negative rate of change of rudder hinge-moment coefficient with rudder deflection and a negative rate of change of rudder hinge-moment coefficient with angle of sideslip. The further deterioration with indicated airspeed is attributable to the effects of Mach number and rudder-tab deflection on these hinge-moment parameters.

INTRODUCTION

A number of military airplanes recently have exhibited poor lateral-oscillation characteristics in high-speed flight. The objectionable motions of the airplane in yaw usually are characterized by constant-amplitude oscillations or by poor damping in conjunction with a short

period. In an effort to determine the causes of these phenomena, the
Ames Aeronautical Laboratory has conducted a detailed investigation of
the dynamic-lateral-stability characteristics of an airplane for which
undesirable oscillatory behavior at high airspeeds had been reported.

At the outset of an investigation of this type there always exists
the question of whether the undesirable damping characteristics are due
to the basic static-stability derivatives (control fixed), the hinge-
moment parameters of the control surfaces (control free), or random
separation phenomena. It was therefore convenient to isolate the effect
of rudder freedom by determining first the dynamic-stability character-
istics with the rudder fixed. These characteristics, which depend
primarily on the combination of basic airplane mass and stability para-
meters, were then analyzed by means of the classic rudder-fixed linearized
equations of motion. The effects of rudder freedom, which are functions
primarily of the rudder mass and hinge-moment derivatives, were determined
and then considered as additional factors or increments which modify the
basic rudder-fixed characteristics.

SYMBOLS

The symbols used in this report are defined in Appendix A.

DESCRIPTION OF AIRPLANE AND INSTRUMENTATION

The airplane on which the tests discussed herein were conducted was
a conventional single-engine low-wing attack airplane. A photograph of
the airplane as instrumented for flight and a three-view drawing are pre-
sented in figures 1 and 2, respectively. Pertinent physical characteris-
tics of the airplane are given in Appendix B.

During the tests the following rudder configurations were tested:

1. Original rudder (fig. 3)
2. Original rudder with trailing-edge bulb on trim tab, as
      used on production version of the airplane (fig. 4)
3. Original rudder with upper horn balance area removed
      (fig. 5)
4. Original rudder with deboost tab (trim tab connected to
      give deboost motion of 1° of tab for 2° of rudder)

Standard NACA recording instruments were used to record the various
quantities presented in this report. The rudder-position recorder, which
was connected directly to the bottom of the rudder structure, permitted
evaluation of the rudder angle to within ±0.1°.

TESTS

Flight Tests

Flight tests were made to determine the lateral—oscillation charac-
teristics of the airplane with the various rudder modifications. The
tests were performed in the 4,000— to 10,000—foot pressure—altitude range
in the power—on clean configuration at various indicated airspeeds from
approximately 200 to 450 miles per hour. The tests were conducted with
a normal center—of—gravity location and with no external stores attached.

Prior to each test run the airplane was trimmed (zero control force)
in steady, straight, wings—level flight. The oscillations were initiated
by release of the rudder control while the airplane was at a moderate
angle of sideslip. The instruments were started just before the release
of the rudder and left on until the oscillations had completely damped or
until approximately 6 cycles were completed. For the rudder—free test
the pilot kept his feet clear of the rudder controls until completion of
the run. For the rudder—locked test the pilot released a locking pin
while in the steady sideslip, and the pin engaged and locked the rudder
when it passed through trim position. This locking mechanism is shown in
figure 6. The ailerons, whether returned to their trim position and held
or left free to oscillate, had no noticeable effect on the yawing motion
of the airplane.

Tests in the Ames 40— by 80—Foot Wind Tunnel

Power—off tests were made in the Ames 40— by 80—foot wind tunnel on
the test airplane to determine the rate of change of rudder hinge—moment
coefficient with rudder deflection C_{h_δ} under conditions similar to those
of the lateral—oscillation flights. The tests were made at an indicated
airspeed of 203 miles per hour at zero yaw with various rudder trim—tab
settings. Both the original rudder and the original rudder with the
trailing—edge bulb were investigated. These data are presented in
figure 7. Values of the rate of change of hinge—moment coefficient with
angle of sideslip C_{h_β} of —0.038 per radian for the original rudder and
—0.045 per radian for the trailing—edge bulb modification were then
derived from steady—sideslip data obtained in flight.

Tests in the Ames 7— by 10—Foot Wind Tunnel

A 0.17—scale powered model of the airplane was tested in the Ames 7—
by 10—foot wind tunnel No. 2 to determine the aerodynamic characteristics
of the model. The rudder used in these tests was similar to the original
rudder configuration of the test airplane, except the rudder tabs were
not adjustable.

The basic aerodynamic parameters obtained from these tests and those estimated by the methods of reference 1 are as follows:

C_{l_p} . . . . −0.43 C_{n_p} . . . . −0.007

C_{l_r} . . . . 0.03 C_{n_β} 0.132

C_{l_β} . . . . −0.08 C_{n_r} . . . . −0.160

C_{Y_β} . . . . −0.802

RESULTS AND DISCUSSION

Figure 8 presents typical time histories of the rudder motion and yawing velocities after a disturbance in yaw for various rudder-control procedures. This figure shows that a rudder-free condition existed even though the pilot attempted to hold the pedals fixed. The movement of the rudder with pedals fixed, though small in magnitude (approximately $\pm 0.3^\circ$ maximum), had an important influence on the damping characteristics of the airplane. The results obtained with this procedure were inconsistent, and are not readily susceptible to analysis by dynamic-stability theory. For the first phase of the investigation, this procedure therefore was discarded in favor of the one in which the rudder was definitely fixed by means of the rudder lock. The characteristics with the rudder-free procedure are considered as the second phase of the investigation.

Rudder-Fixed Characteristics

The results of the rudder-fixed oscillation flight tests are summarized in figure 9, in which period P, time to damp to one-half amplitude $T_{\frac{1}{2}}$, and cycles to damp to one-half amplitude $C_{\frac{1}{2}}$ are plotted as a function of indicated airspeed. Plotted on this same figure for the purpose of comparison are the computed values[1] of the three parameters at

[1]In most theoretical investigations, the effect of the product-of-inertia terms resulting from the inclination of the principal longitudinal axis of the airplane has been considered small. However, Sternfield recently has shown in reference 2 that neglect of these terms can lead to considerable error in the prediction of the oscillatory divergency boundaries for modern airplanes. Computations for the test airplane based on the equations of reference 3, which include the effect of the product-of-inertia terms, give the value of 0.75 for $C_{\frac{1}{2}}$ shown in figure 9. A value of 0.67 was calculated by the method of reference 4 which neglects these terms. Inclusion of the product-of-inertia terms had negligible effect on the computed period for the test airplane.

an airspeed of 210 miles per hour and an extrapolation of these character-
istics to higher speeds based on the assumption of a constant value of the
stability derivatives throughout the speed range.

In view of the deterioration in damping at higher speeds, observed
with rudder free (to be discussed later), it was considered possible that
there might be a significant Mach number effect on the stability deriva-
tives. The fact that this is not so over the Mach number range of the
flight tests with regard to any of the stability derivatives which affect
the rudder—locked oscillation is shown by the comparison of the variation
of the experimental and theoretical characteristics with airspeed in
figure 9. The inverse variation of P and $T_{\frac{1}{2}}$ with speed and the con-
stant value of $C_{\frac{1}{2}}$ shown in this figure is in accordance with the control—
locked stability equations for a constant value of the stability deriva-
tives. The correspondence between the experimental and predicted oscilla-
tion characteristics over the range of the tests is considered to be
within the experimental accuracy, an indication that the assumption of a
constant value of the stability derivatives over the Mach number range
was a sound one and that there are no unaccounted factors affecting the
oscillation characteristics with rudder fixed. From this it is concluded
that the poor damping characteristics of the test airplane arise from the
rudder hinge—moment characteristics.

Rudder—Free Characteristics

During the rudder—free flight tests, three types of yawing oscilla-
tions were encountered. These oscillations have been termed completely
damped, incompletely damped, and increasing amplitude. Typical yawing—
velocity records of these types are presented in figure 10. The damping
characteristics derived from records of this type for the various rudder
modifications are summarized in figure 11.

In order to compare the experimental results with those predicted
from the values of the rudder hinge—moment parameters produced by the
various rudder modifications, the variation of the damping characteristics
of the test airplane for a range of values of C_{h_β} and C_{h_δ} has been
computed by the basic method of reference 4.[2] Figure 12 shows the boun-
daries for the various types of lateral oscillation and figure 13 shows
the variation of the period and cycles to damp to one—half amplitude com-
puted by this method.

---

[2]The computations were made by the simplified method of reference 5, as
    outlined in Appendix C, which makes practical the consideration of the
    effects of product—of—inertia terms.

The values of C_{h_δ} and C_{h_β} at a speed of 203 miles per hour were available from the 40- by 80-foot wind-tunnel tests and the flight tests for the original rudder and for the original rudder with a trailing-edge bulb. Application of these data at the tab setting used in flight for the wings level, trimmed condition (2.2° left for the original rudder and 0.8° left for the original rudder with trailing-edge bulb) results in the following comparison between the predicted and measured oscillation characteristics.

Rudder configuration	Flight Tests		Predicted from full-scale C_h data	
	Period (sec)	Cycles to one-half amplitude	Period (sec)	Cycles to one-half amplitude
Original rudder	2.13	1.75	1.95	1.35
Trailing-edge bulb modification	2.30	1.15	2.03	1.01

In the case of the original rudder with trailing-edge bulb, the comparison between the computed and measured damping is good. The likely reason for the less satisfactory agreement in the case of the original rudder is evident from figure 13, which shows that with the small value of C_{h_δ} existent on the original rudder, a small inaccuracy in the evaluation of C_{h_δ} or C_{h_β} would cause appreciable changes in the cycles to damp to one-half amplitude. Another source of error not evident from this figure is inaccuracy in the evaluation of the rudder damping parameter[3] $C_{h_{D_\delta}}$.

This term, which is relatively unimportant when C_{h_δ} is high, increases in importance at the lower values of C_{h_δ} and can significantly affect the location of the knee of the curves of figure 13(a). It can be concluded from the foregoing that the lateral-oscillation characteristics can be satisfactorily predicted by available methods, provided the combination of hinge-moment parameters is not such as to put the airplane in the knee or beyond the knee of the curves of figure 13(a).

---

[3]The value of $C_{h_{D_\delta}}$ of -0.154 used in this investigation was obtained from reference 6.

The important influence of tab setting is evident from figure 7. The change in C_{h_δ} between $\pm 4°$ tab setting is sufficient to increase the cycles to damp to one-half amplitude as much as 50 percent on the original rudder and 10 percent on the rudder with the trailing-edge bulb as shown in figure 13(a). This effect was exemplified in flight, as indicated by the curves in figure 11. Above 400 miles per hour, the damping characteristics are considerably inferior for the out-of-trim tab setting, in comparison with the characteristics for the in-trim tab setting. It is evident that a conservative design must allow a reasonable margin for these changes in C_{h_δ} due to tab setting, if undesirable damping characteristics are to be avoided.

No quantitative data were available on C_{h_δ} and C_{h_β} with the deboost tab or the horn-removed modifications. However, it is known that the former modification will increase C_{h_δ} negatively and the latter will increase C_{h_β} positively and C_{h_δ} negatively. Both these changes are such as to move the rudder characteristics into the better damping range. Figure 11 shows that the flight results are in conformity with this trend. The deboost tab modification is of special interest, since it furnishes an expedient by which a rudder which has an undesirable C_{h_δ} and C_{h_β} combination, insofar as damping is concerned, can readily be adjusted for more favorable characteristics.

On all of the rudder modifications tested, except with the upper horn modification, there is observed a gradual deterioration of the damping of the airplane with speed. As previously mentioned, the rudder-fixed tests show that this deterioration is not traceable to any control-fixed stability parameters. It can be inferred, therefore, that the effect is due to a change in C_{h_δ} and C_{h_β} with Mach number. No experimental data are available to verify this inference on the rudder used on the test airplane, but this trend has been observed in high Mach number tests of other control surfaces. In particular, if the trailing-edge angle is large, it can be anticipated that C_{h_δ} will increase positively and C_{h_β} will increase negatively with Mach number, a trend which figure 13 shows will move the rudder into the decreased damping range. Sound design practice, therefore, calls for an allowance for changes of this type in selecting the low-speed parameters by methods of references 4 and 5.

CONCLUDING REMARKS

The current trend of airplane design which leads to intentional selection of a low rate of change of rudder hinge-moment coefficient with rudder deflection C_{h_δ} and a negative rate of change of rudder hinge-moment

coefficient with angle of sideslip C_{h_β} is such as to invite increasing

amplitude or poorly damped oscillations. It is therefore important that the damping characteristics be checked by the methods of Greenberg and Sternfield or, if product—of—inertia terms are found to be important, by the methods of Neumark. Allowances should be made for the effect of tab deflection and Mach number on the hinge—moment parameters.

Ames Aeronautical Laboratory,
    National Advisory Committee for Aeronautics,
        Moffett Field, Calif., Dec. 19, 1947.

APPENDIX A

SYMBOLS

S	wing area, square feet
V	free-stream airspeed, feet per second
V_i	indicated airspeed, miles per hour
b	wing span, feet
b_r	span of rudder, feet
m	mass of the airplane, slugs
m_r	mass of the rudder, slugs
k_Z	radius of gyration of airplane about vertical (Z) axis, feet
k_r	radius of gyration of rudder about hinge axis, feet
P	period of oscillations, seconds
$T_{\frac{1}{2}}$	time required for motions to decrease to one-half amplitude, seconds
$C_{\frac{1}{2}}$	cycles required for motions to decrease to one-half amplitude
t	time, seconds
$A,B,C,$ E,F	coefficients of the rudder-free lateral-stability equation
f,h	coefficient of the rudder-fixed quadratic factor $\lambda^2 + f\lambda + h$ for which the roots correspond to the apparent lateral oscillation
λ	root of the stability determinant
ib'	imaginary portion of complex root of the stability determinant
a'	real portion of the complex root of the stability determinant

q dynamic pressure, pounds per square foot $\left(\frac{1}{2}\rho V^2\right)$

ρ mass density of air, slugs per cubic foot

μ airplane relative-density factor $(m/\rho Sb)$

μ_r rudder relative-density factor $(m_r/\rho b_r \bar{c}_r^2)$

$\bar{c}_r$ mean aerodynamic chord of rudder, feet

β angle of sideslip, radians

δ rudder deflection, radians

r yawing angular velocity, radians per second

C_Y lateral-force coefficient (lateral force/qS)

C_n yawing-moment coefficient (yawing moment/qSb)

C_l rolling-moment coefficient (rolling moment/qSb)

C_h hinge-moment coefficient (hinge moment/$qb_r\bar{c}_r^2$)

C_{n_β} rate of change of yawing-moment coefficient with angle of sideslip $(\partial C_n/\partial\beta)$

C_{Y_β} rate of change of lateral-force coefficient with angle of sideslip $(\partial C_Y/\partial\beta)$

C_{l_r} rate of change of rolling-moment coefficient with yawing angular-velocity factor $\left[\partial C_l/\partial(rb/2V)\right]$

C_{l_p} rate of change of rolling-moment coefficient with rolling angular-velocity factor $\left[\partial C_l/\partial(pb/2V)\right]$

C_{l_β} rate of change of rolling-moment coefficient with angle of sideslip $(\partial C_l/\partial\beta)$

C_{n_r} rate of change of yawing-moment coefficient with yawing angular-velocity factor $\left[\partial C_n/\partial(rb/2V)\right]$

C_{n_δ} rate of change of yawing-moment coefficient with rudder deflection $(\partial C_n/\partial\delta)$

C_{h_β} rate of change of rudder hinge-moment coefficient with angle of sideslip $(\partial C_h/\partial\beta)$

C_{h_r} rate of change of rudder hinge—moment coefficient with

yawing angular—velocity factor $\left[\partial C_h / \partial (rb/2V) \right]$

C_{h_δ} rate of change of rudder hinge—moment coefficient with
        rudder deflection $(\partial C_h / \partial \delta)$

$C_{h_{D_\delta}}$ rate of change of rudder hinge—moment coefficient with

rudder angular—velocity factor $\left\{ \partial C_h / \partial \left[\dfrac{(d\delta/dt)b}{2V} \right] \right\}$

APPENDIX B

PHYSICAL CHARACTERISTICS OF THE TEST AIRPLANE

General

Test gross weight . . . . 13,000 lb
Moment of inertia in yaw
  about principal axis . . . . 36,340 slug—ft^2
Moment of inertia in roll
  about principal axis . . . . 13,980 slug—ft^2
Angle between reference
  axis and principal axis,
  positive when reference axis is
  above principal axis at nose . . . . 2.4°
Distance from airplane center of
  gravity (0.25 M.A.C.) to rudder
  hinge line . . . . 23.0 ft

Wing

Area . . . . 400 sq ft
Span . . . . 50.0 ft
Aspect ratio 6.25
Taper ratio 0.503
Mean aerodynamic chord . . . . 8.34 ft
Dihedral . . . . 6.0°
Incidence (root—chord station 30) . . . . 3.97°
Geometric twist . . . . 4.22°
Root section . . . . NACA 2417 (station 30)
Tip section . . . . NACA 4413 (station 300)

Vertical tail

Area . . . . 35.01 sq ft
Span . . . . 7.67 ft

Aspect ratio 1.68
Taper ratio 0.549
Mean aerodynamic chord . . . . 4.78 ft
Offset . . . . 3.0° from station 45 to tip
Root section . . . . NACA 0013.44—64 modified to
                                                        12—percent thickness
Tip section . . . . NACA 0012—64 modified to 10.71—
                                                              percent thickness

Rudder

Area aft of hinge line . . . . 18.99 sq ft
Span . . . . 9.67 ft
Mean aerodynamic chord . . . . 2.08 ft
Chord aft of hinge line, percent
    fixed surface chord 40
Total balance area
    Original rudder . . . . 4.82 sq ft
    Original rudder with the upper
        horn removed . . . . 3.79 sq ft
Nose gap . . . . fabric sealed
Contour aft of hinge line . . . . straight
Travel . . . . (approximately) ± 25°
Included trailing—edge angle . . . . 13°

Tabs

Trim
    Area aft of hinge line . . . . 1.91 sq ft
    Span . . . . 4.08 ft
    Chord, percent of control chord 6.99
    Travel . . . . (approximately) ±10°
    Balance ratio (tab throw
        per surface throw)
            Original rudder 0
            Deboost modification 0.5

Spring
    Area aft of hinge line 1.00
    Span . . . . 2.59 ft
    Chord, percent of control chord 7.01
    Travel . . . . (approximately) ±15°
    Spring constant, rudder
        hinge moment per tab angle . . . . 5.78 ft—lb
                                                              per degree

Moment of inertia of the rudder
    system about hinge line . . . . 2.27 slug—ft^2
Rudder frictional hinge moment . . . . 1.2 ft—lb

Engine

Type . . . . Wright R–3350–8
Propeller gear ratio 0.4375
Normal horse power ratings
   Sea level . . . . 2100 hp at 2400 rpm
   3800 feet . . . . 2100 hp at 2400 rpm

Propeller

Type . . . . Curtiss Electric
Number of blades . . . . four
Diameter . . . . 13 ft 0 in.
Blade design X836–14C2–18R1
                                     cuffs removed

APPENDIX C

CALCULATION METHODS

The method employed in the present investigation for predicting the rudder–free dynamic lateral stability of the airplane was taken from reference 5. It makes use of the coefficients of the rudder–locked quadratic factor $\lambda^2 + f\lambda + h$, for which the roots correspond to the motion which is readily apparent to the pilot. The substance of this procedure is the neglecting of the effect of C_{Y_β} on rudder–motion terms during the determinant expansion process while retaining C_Y effects on other terms. Application of this procedure, using rudder–fixed coefficients and not considering rolling, yields an equation of the form:

$$A\lambda^4 + B\lambda^3 + C\lambda^2 + E\lambda + F = 0 \tag{1}$$

where

$A = 1$

$$B = f - \frac{C_{h_{D_\delta}}}{4\mu_r}\left(\frac{b}{k_r}\right)^2$$

$$C = h + \frac{C_{n_\delta}}{2\mu}\left(\frac{b}{k_Z}\right)^2 - \frac{C_{h_\delta}}{2\mu_r}\left(\frac{b}{k_r}\right)^2 - \frac{f\left(C_{h_{D_\delta}}\right)}{4\mu_r}\left(\frac{b}{k_r}\right)^2 + \frac{l\overline{x}_r C_{n_\delta}}{2\mu(k_Z)^2}\left(\frac{b}{k_r}\right)^2$$

$$E = \frac{f\left(C_{h_\delta}\right)}{2\mu_r}\left(\frac{b}{k_r}\right)^2 - \frac{h\left(C_{h_{D\delta}}\right)}{4\mu_r}\left(\frac{b}{k_r}\right)^2 - \frac{C_{h_r}C_{n_\delta}}{8\mu\mu_r}\left(\frac{b}{k_Z}\right)^2\left(\frac{b}{k_r}\right)^2$$

$$F = \frac{C_{h_\beta}C_{n_\delta}}{4\mu_r\mu}\left(\frac{b}{k_r}\right)^2\left(\frac{b}{k_Z}\right)^2 - \frac{h\left(C_{h_\delta}\right)}{2\mu_r}\left(\frac{b}{k_r}\right)^2$$

The roots of equation (1) which define the apparent lateral oscilla-
tions are of the form $\lambda = a' + ib'$. These roots are used in the follow-
ing equations to determine the period and time to damp to one-half ampli-
tude:

$$P = \frac{2\pi}{b'}\frac{b}{V} \tag{2}$$

$$T_{\frac{1}{2}} = \frac{-\log_e 0.5}{a'} \tag{3}$$

The relationship between C_{h_δ} and C_{h_β} which defines the boundary
for divergence is obtained by setting $F = 0$ and that for oscillations
of increasing amplitude is found by setting Routh's discriminant

$$R = BCE - AE^2 - FB^2 = 0$$

The incomplete damping boundary, which defines a region between
damped and increasing-amplitude oscillations in which constant-amplitude
oscillations occur, is the envelope of the boundaries for increasing
oscillations for various values of $C_{h_{D\delta}}$.

The coefficients f and h of the rudder-locked quadratic factor,
which are used in the present investigation, were obtained from the rudder-
locked flight-test data presented in figure 9. By the use of the quadratic
formula, equations (2) and (3) can be transformed for the rudder-locked
case to the form

$$f = \frac{2\log_e 0.5}{T_{\frac{1}{2}}}\frac{b}{V} \tag{4}$$

and

$$h = \frac{4\pi^2}{P^2}\frac{b^2}{V^2} + \frac{f^2}{4} \tag{5}$$

Values of $T_{\frac{1}{2}}$, P, and V from figure 9 can then be substituted in
equations (4) and (5) to evaluate f and h. Rudder-locked oscillation

flight—test data usually are not available for use in the prediction of rudder—free characteristics. In that case, a' and b' (and hence f and h) can be evaluated from wind—tunnel data or other information by a method such as that given in reference 3, in which the effects of rolling and the product of inertia due to the inclination between the wind axis and the principal axis are considered.

REFERENCES

1. Pearson, Henry A., and Jones, Robert T.: Theoretical Stability and
   Control Characteristics of Wings With Various Amounts of Taper and
   Twist. NACA Rep. 635, 1938.

2. Sternfield, Leonard: Effect of Product of Inertia on Lateral
   Stability. NACA TN 1193, 1947.

3. Sternfield, Leonard: Some Considerations of the Lateral Stability
   of High-Speed Aircraft. NACA TN 1282, 1947.

4. Greenberg, Harry, and Sternfield, Leonard: A Theoretical Investiga-
   tion of the Lateral Oscillations of an Airplane with Free Rudder
   with Special Reference to the Effect of Friction. NACA Rep. 762, 1943

5. Neumark, S.: A Simplified Theory of the Lateral Oscillations of an
   Aircraft with Rudder Free, Including the Effect of Friction in the
   Control System. R. & M. No. 2259 (British), May 1945.

6. Jones, Robert T., and Cohen, Doris: An Analysis of the Stability of
   an Airplane with Free Controls. NACA Rep. 709, 1941.
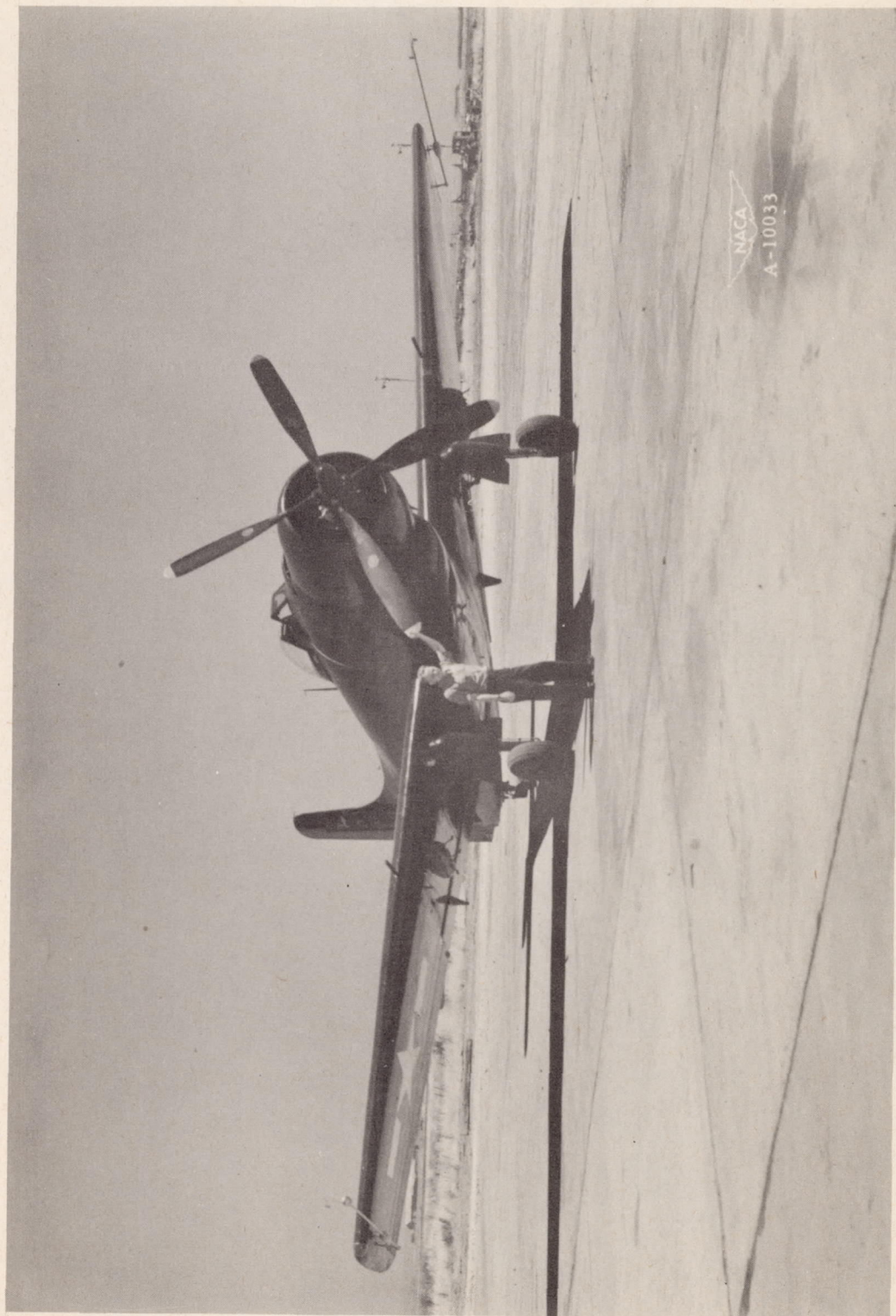
Figure 1.— The test airplane instrumented for flight.
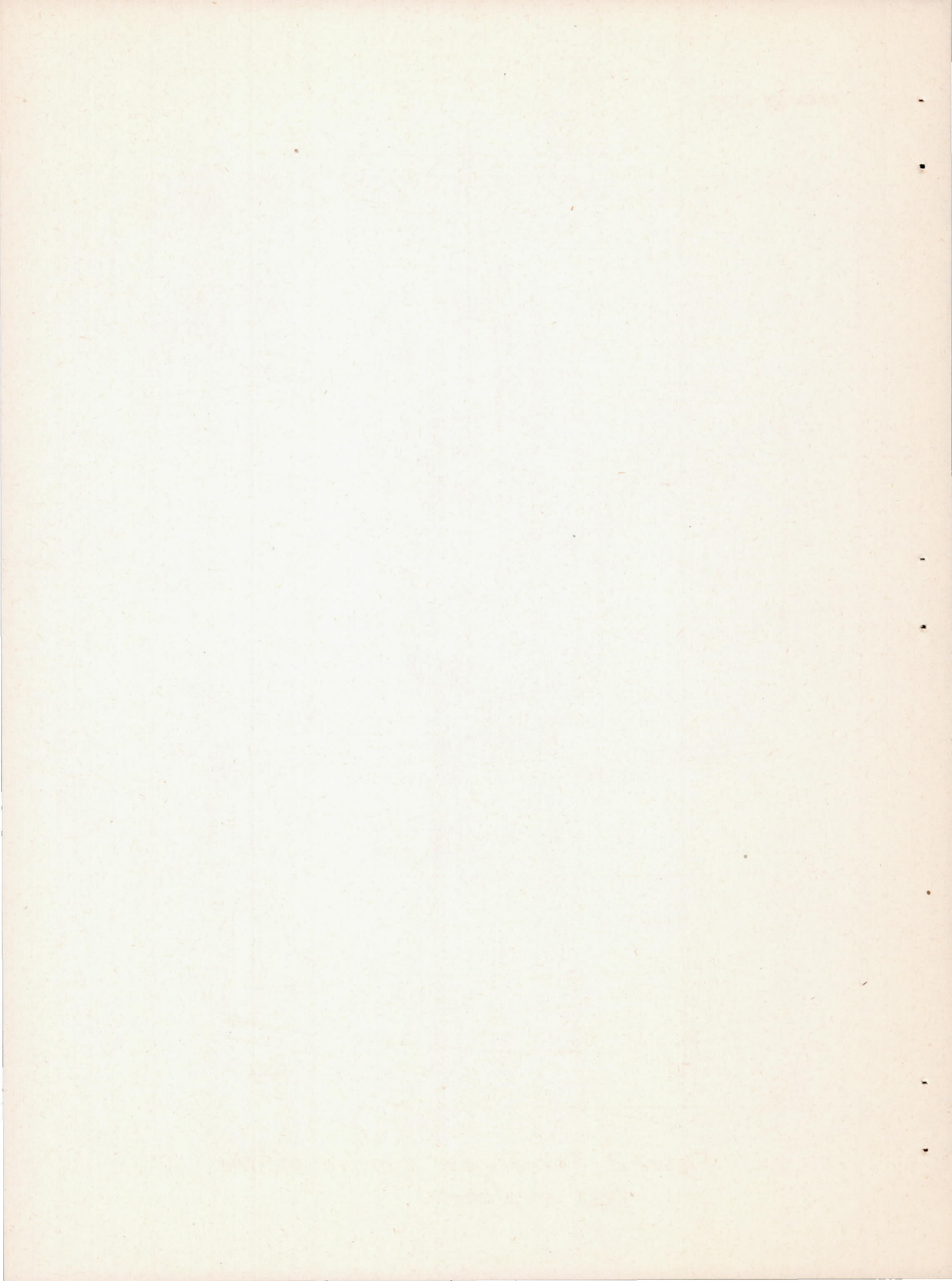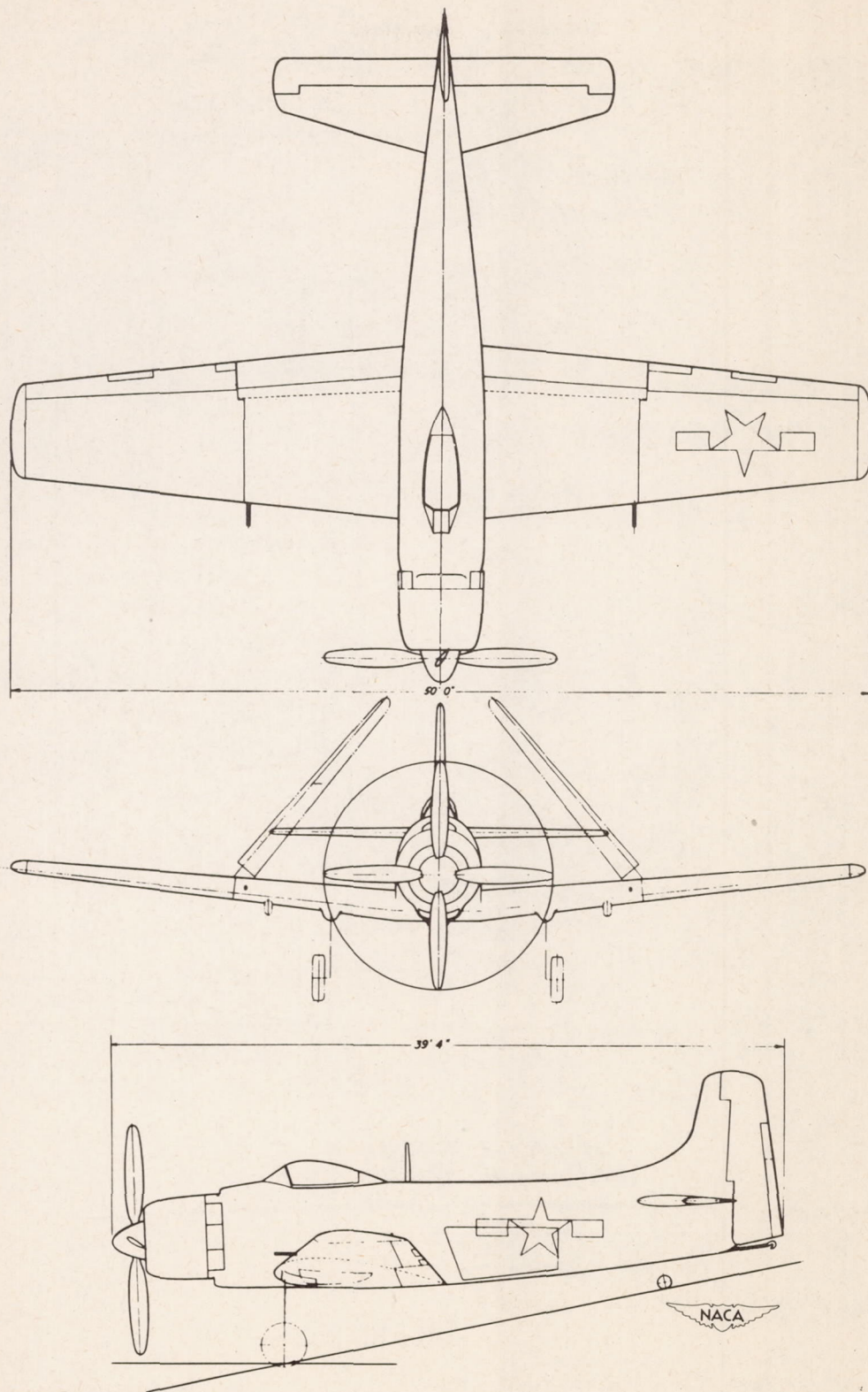
Figure 2.- Three-view drawing of the
test airplane.

All dimensions in inches

Shielded
horn balance

Sealed over-
hang balance

39.34

12.39 | 15.73

20.0

57.0

31.12

Spring tab

Trim and boost tab

122.0

A
sta.45

48.0

Unsealed
radius nose

Fuselage
ref. line

82.25   32.90

Fin offset 3° nose
left above sta 45

Airplane
C̶L

Fuselage-dorsal lines

Section A-A

NACA
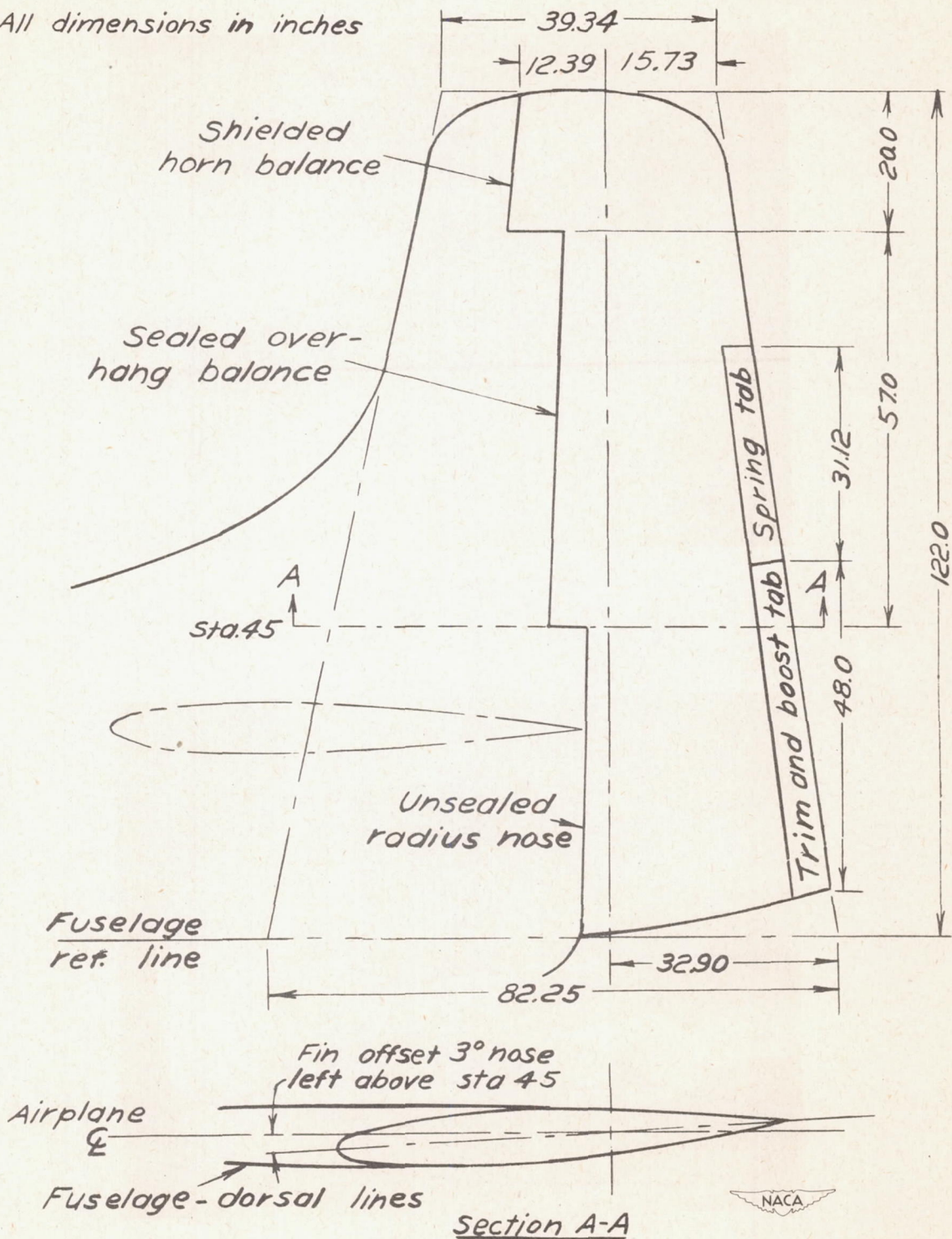
Figure 3. – Vertical tail with the original
rudder.
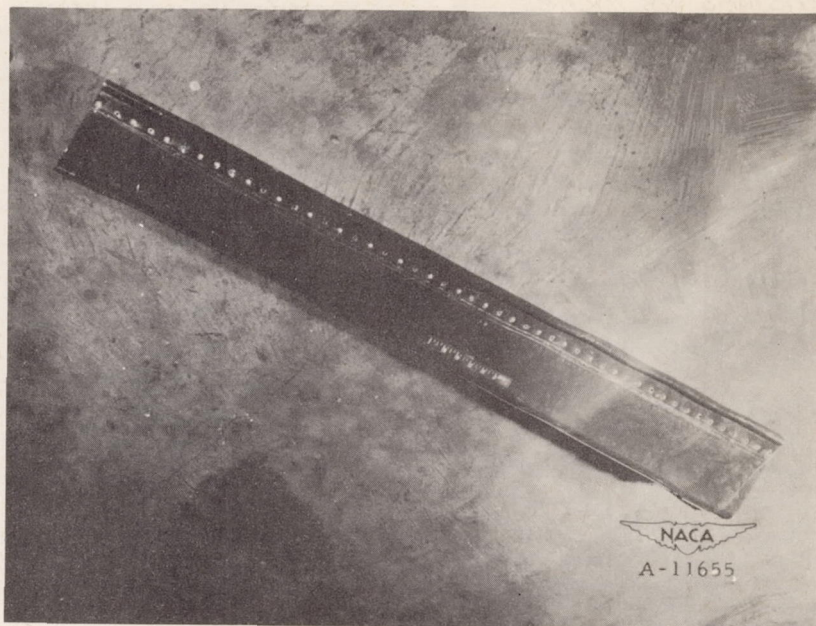
(a) Top view.
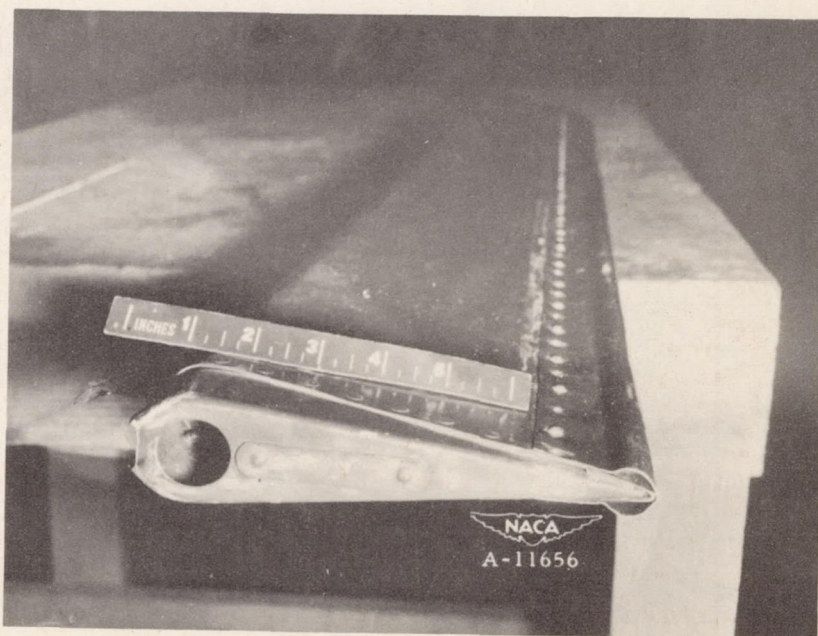
(b) End view.

Figure 4.— Rudder trim tab with the trailing-edge bulb attached.
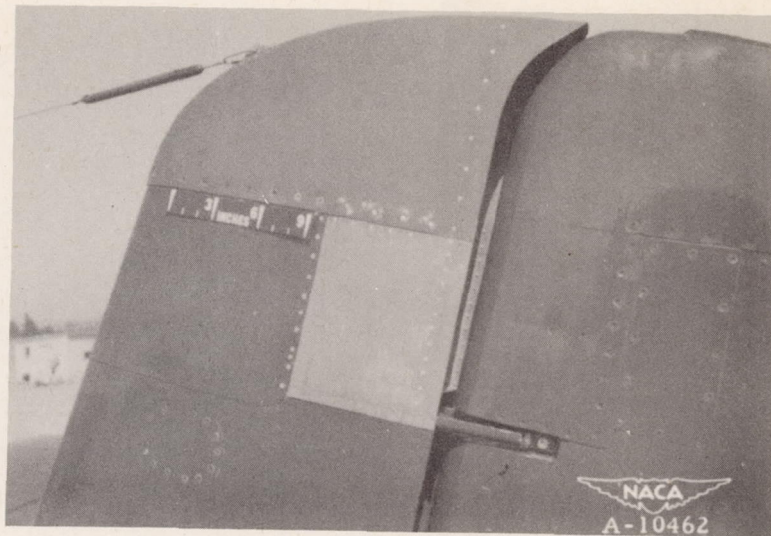
(a) Close up.

(b) Side view.

Figure 5.— Vertical tail with the horn—balance area removed from
the rudder.
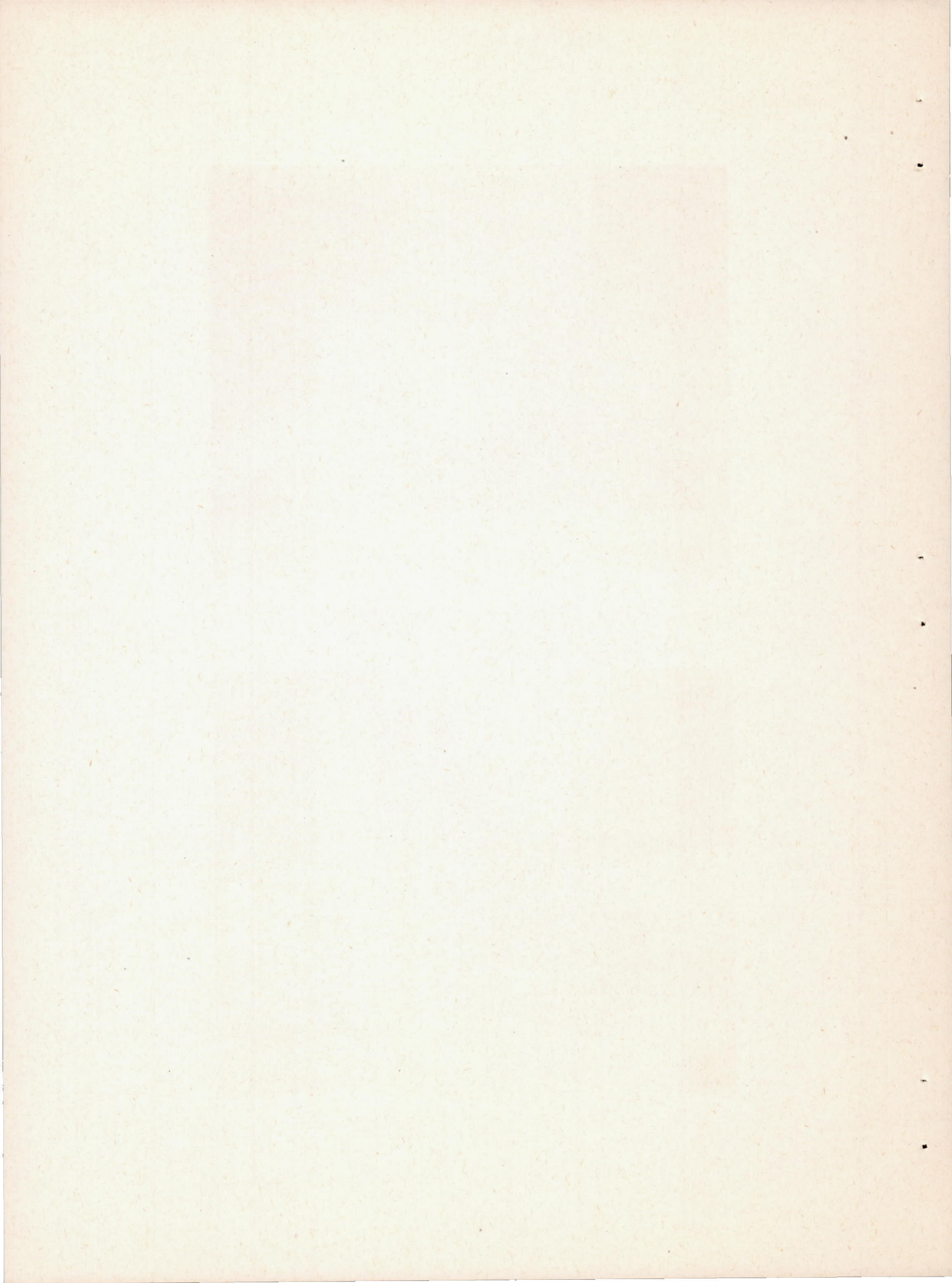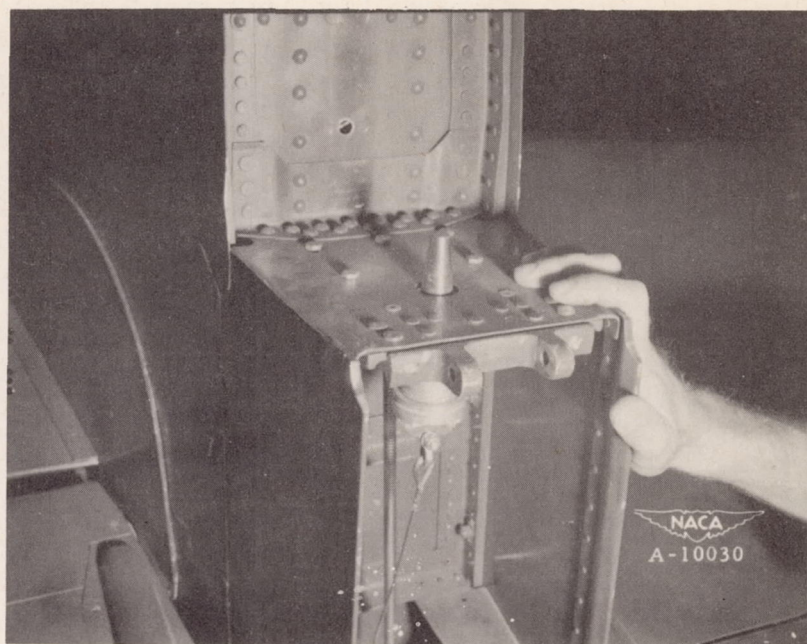
(a) Three-quarter rear view.
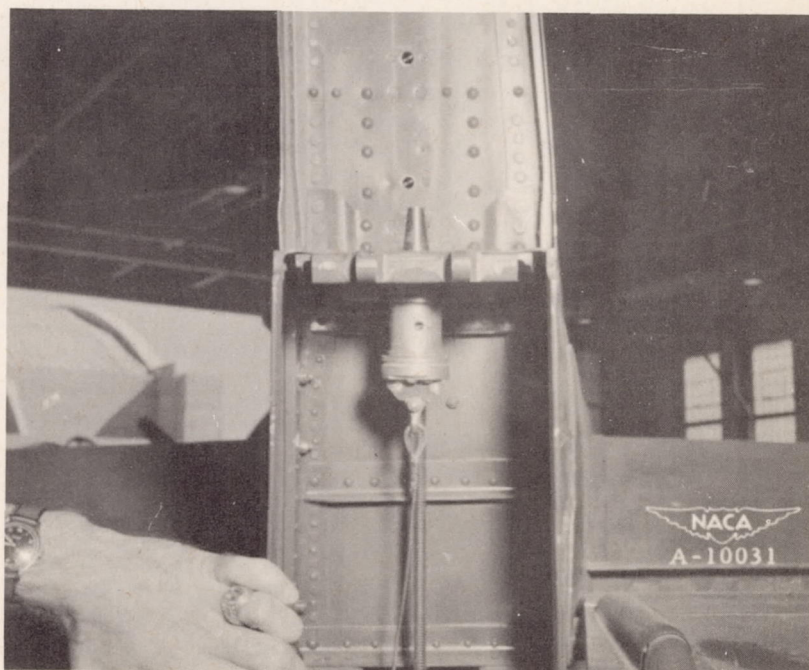
(b) Rear view.

Figure 6.— Mechanism for locking the rudder.
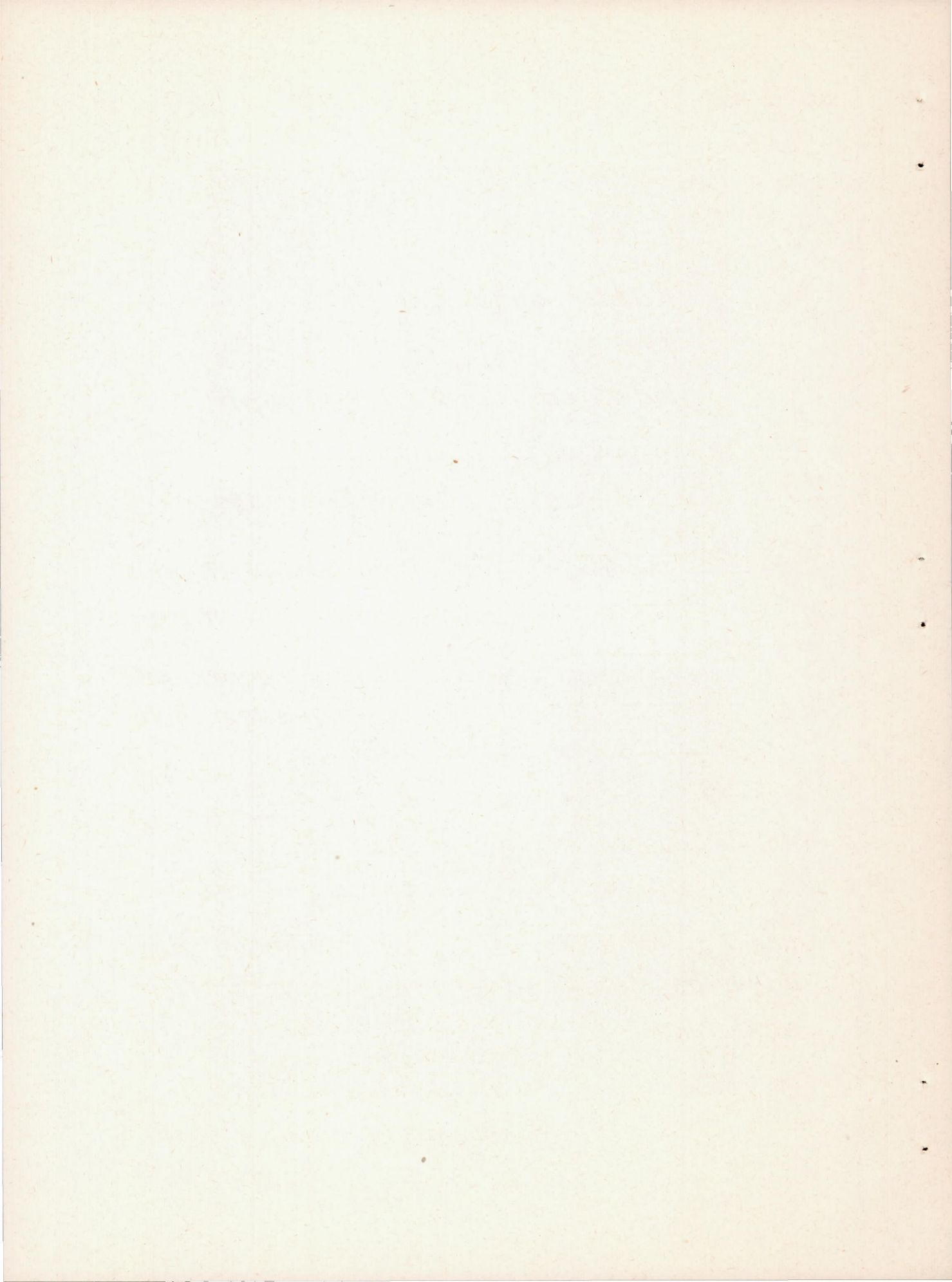
Rudder angle 2.5° left
Yaw 0°
Indicated airspeed 203 mph
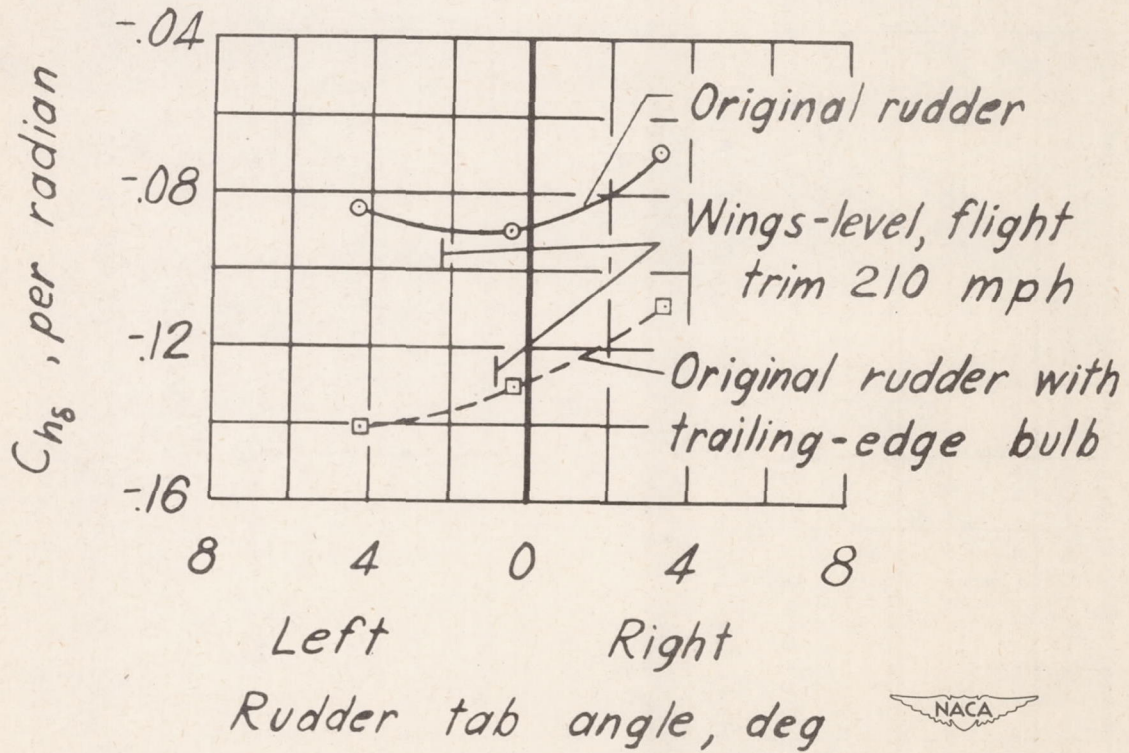
Figure 7.- Variation of C_{h_δ} with rudder tab
angle as measured in the 40- by 80- foot
wind tunnel.
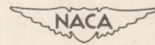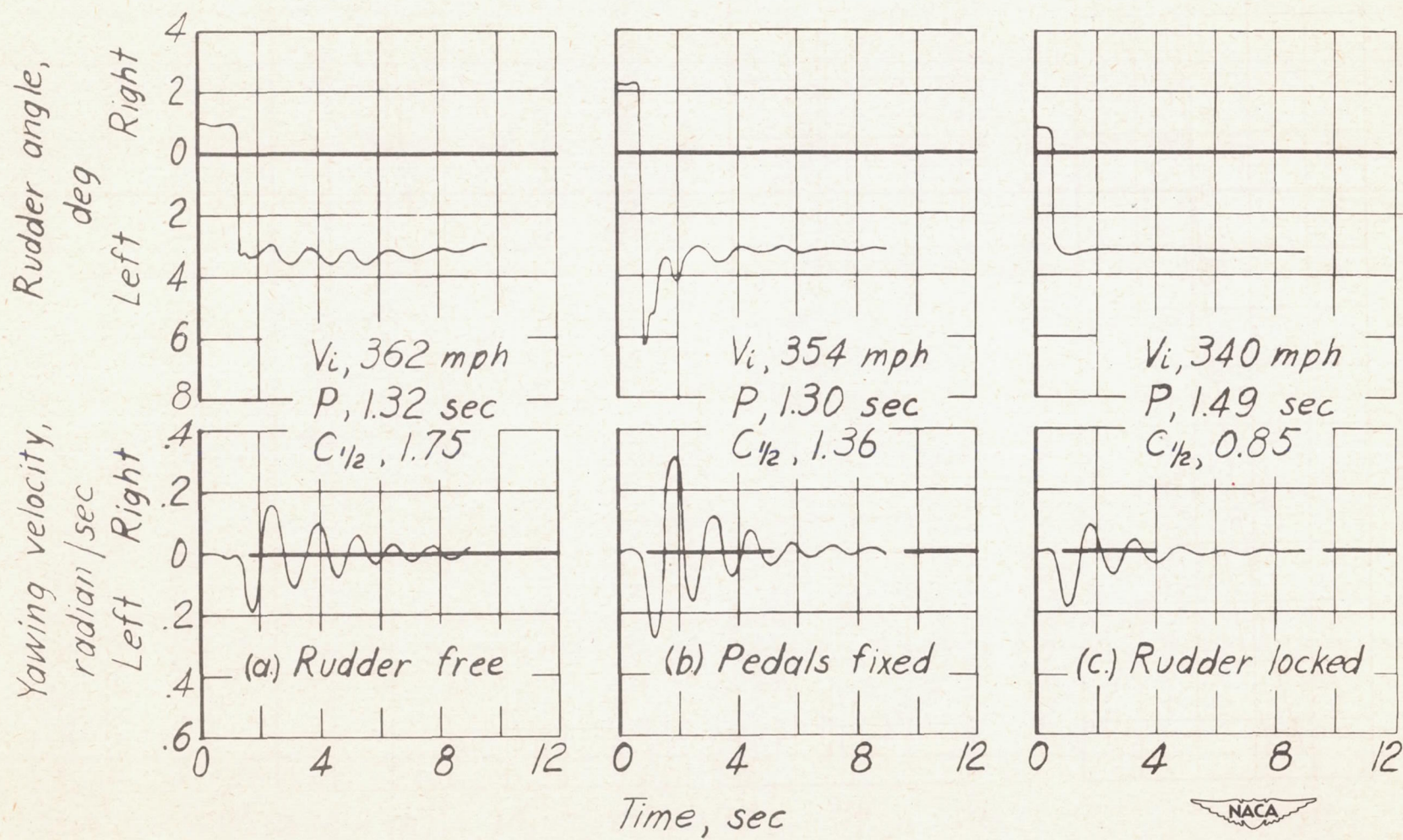
Figure 8.- Time histories showing the effect of rudder-control procedure on lateral-oscillation characteristics.
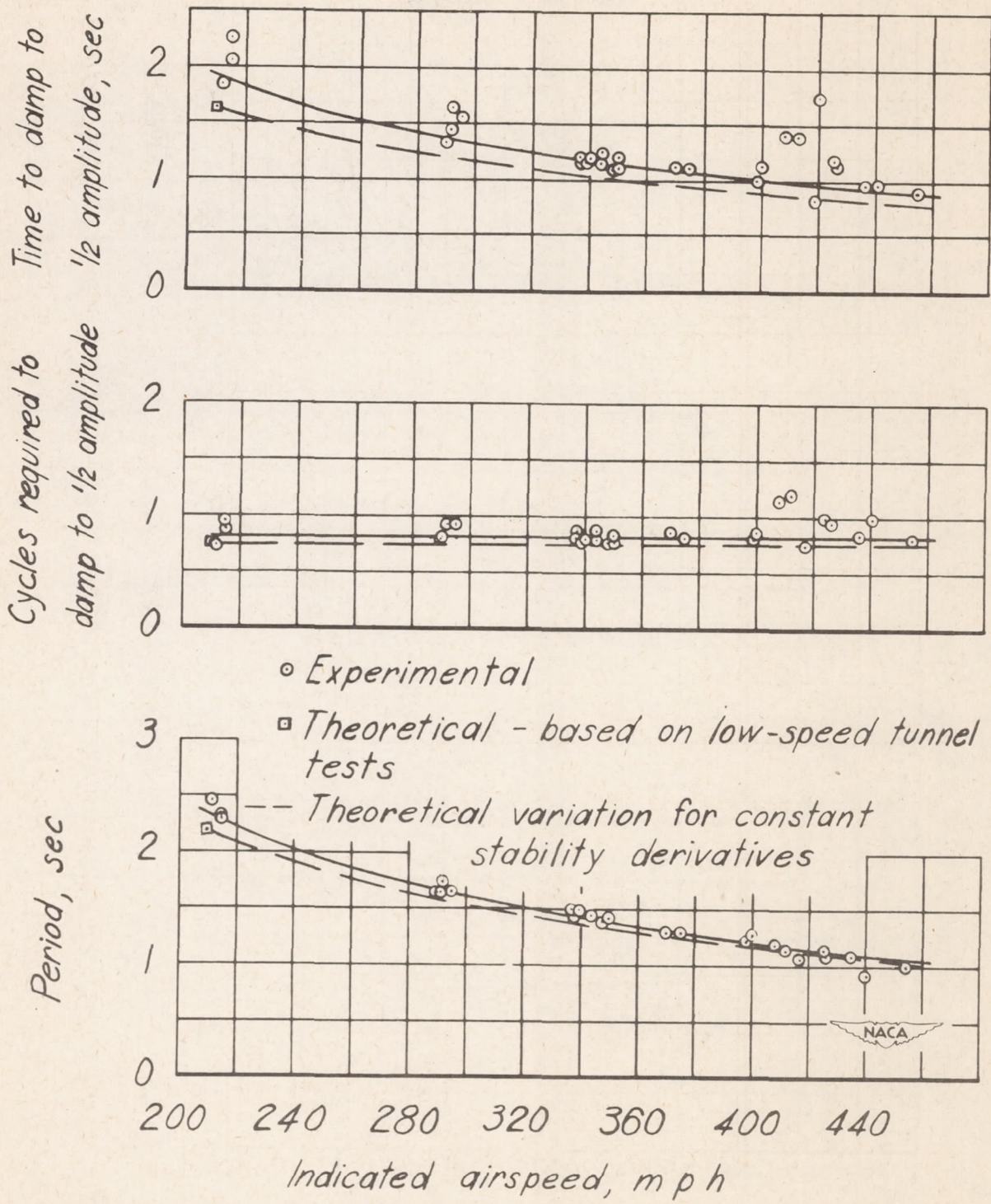
Figure 9.- Variation of period and damping with air-
speed, rudder locked.
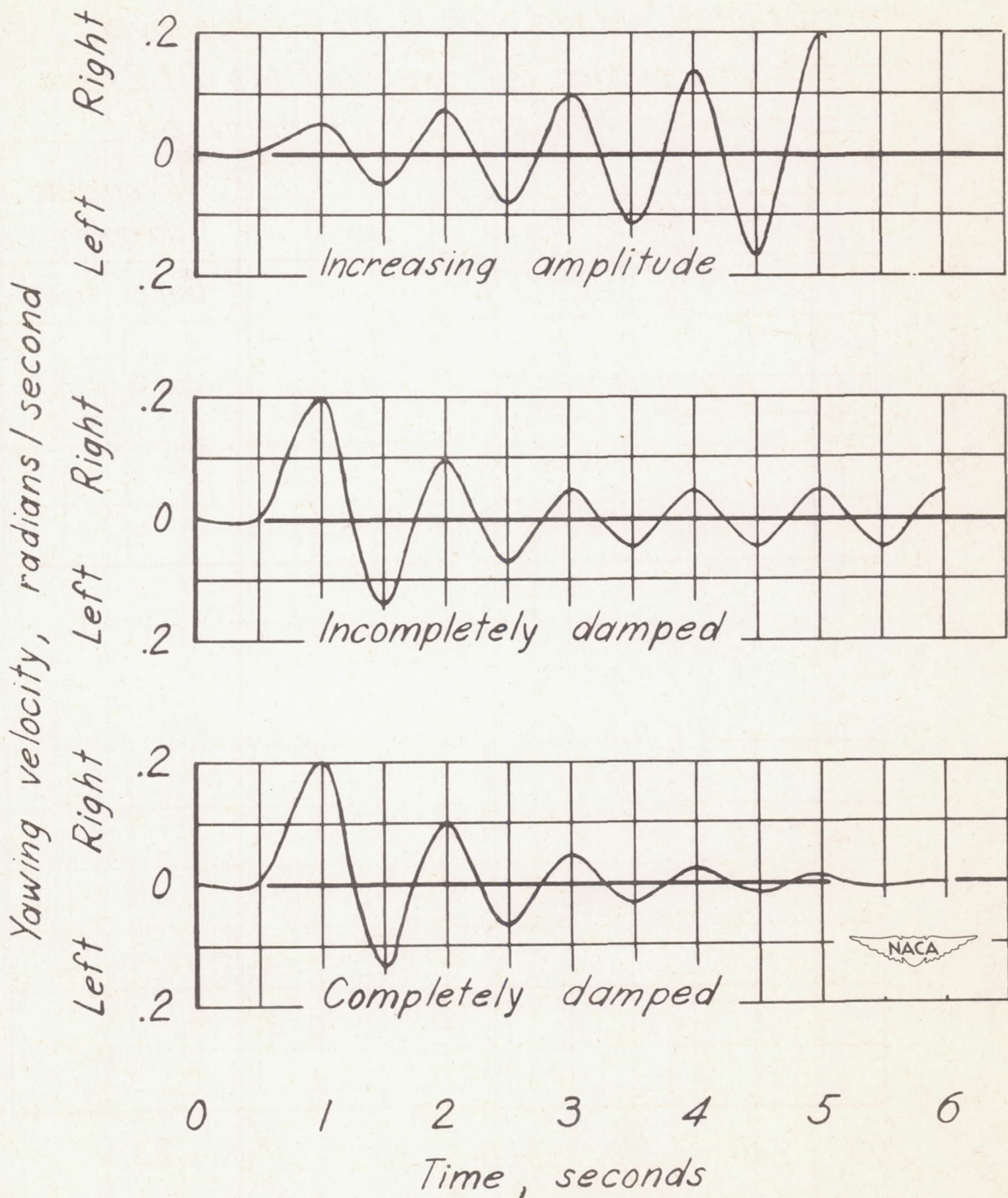
Figure 10- Typical yawing-velocity time histories
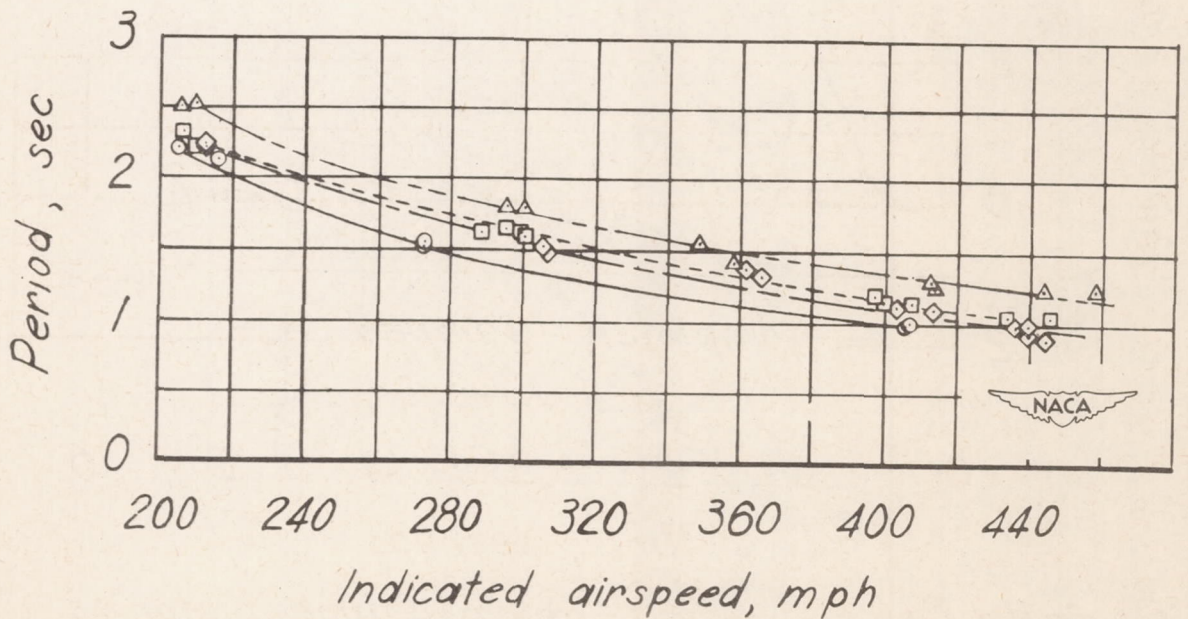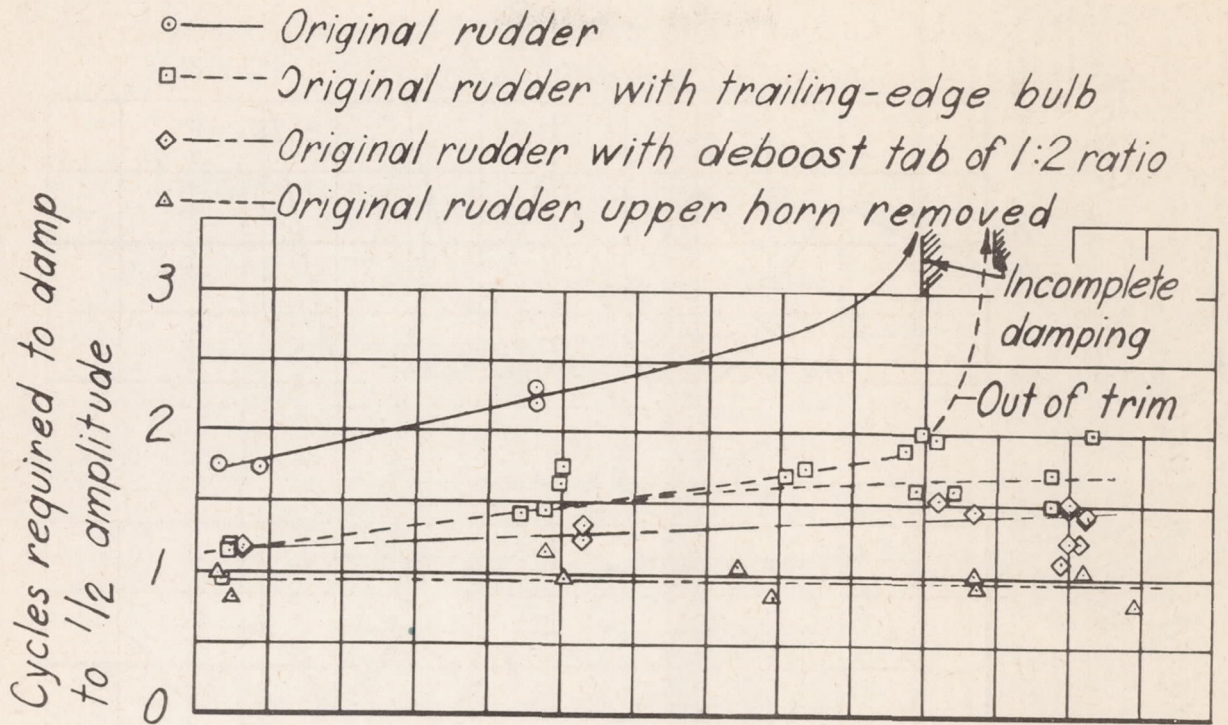of the various types of oscillations encountered.

Figure 11.- Variation of period and damping with airspeed, rudder free.

⊙ Original rudder, full-scale data
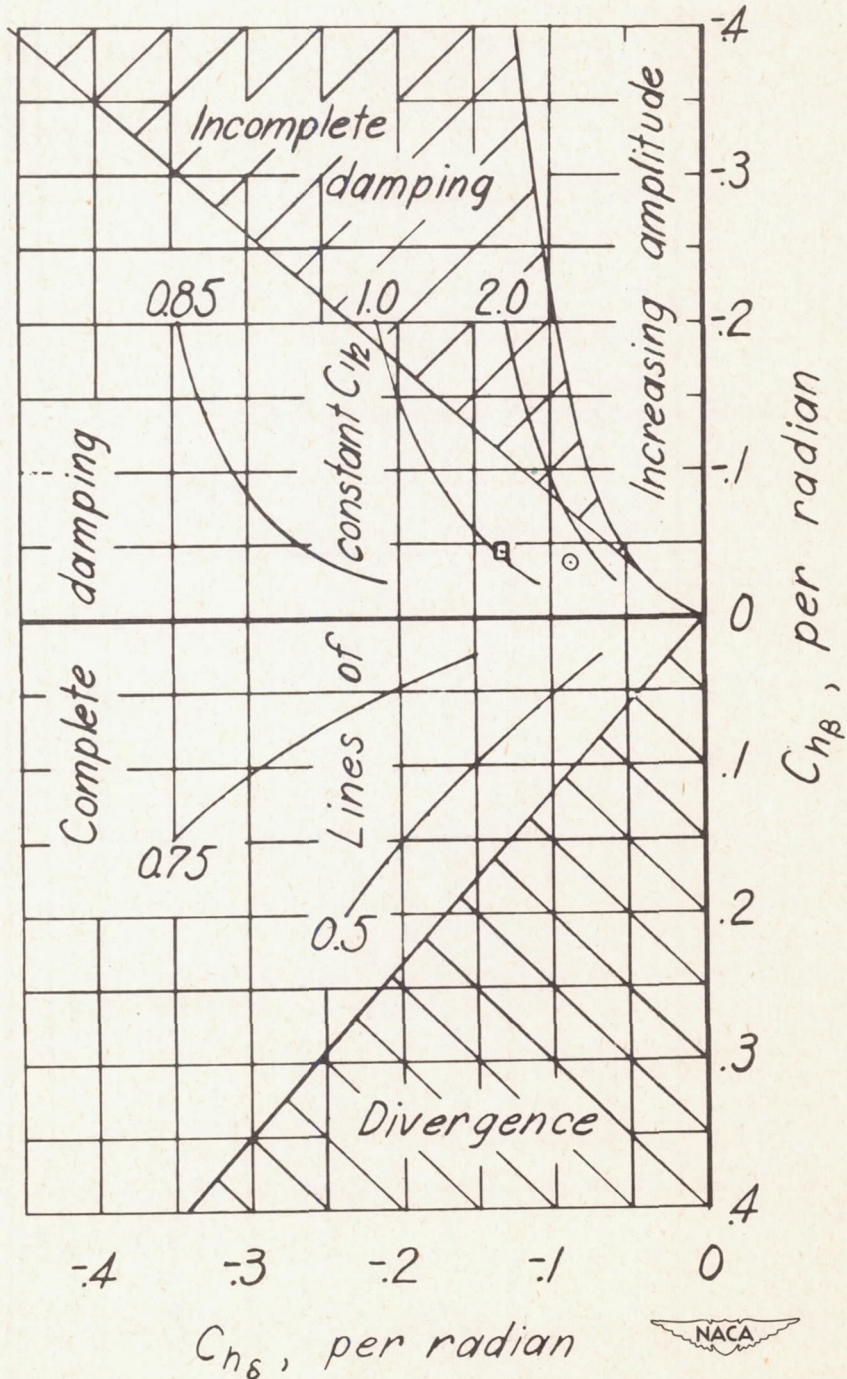□ Trailing-edge bulb modification, full-scale data

Figure 12.- Boundaries for the various types of rudder-free lateral oscillations.
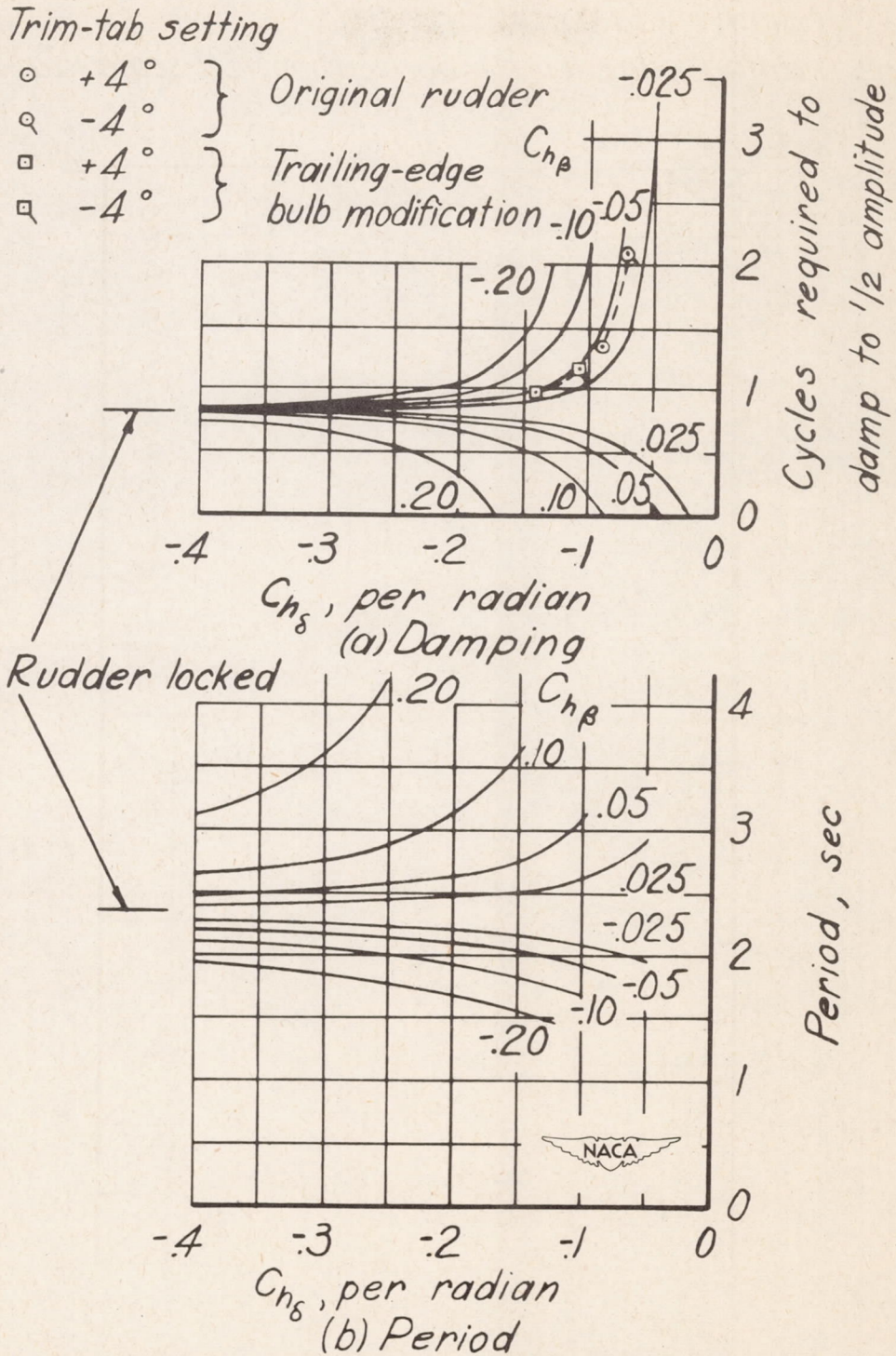
Trim-tab setting

⊙ +4° } Original rudder

⊘ -4°

▢ +4° } Trailing-edge

▫ -4° } bulb modification

(a) Damping

C_{h_δ}, per radian

Rudder locked

(b) Period

C_{h_δ}, per radian

Figure 13.- Variation of period and damping with C_{h_δ} for various values of C_{h_β}; V_i, 210 mph.